Avrupa Bilim ve Teknoloji Dergisi
Sayı 23, S. 359-367, Nisan 2021

Araştırma Makalesi

www.ejosat.com ISSN:2148-2683

European Journal of Science and Technology
No. 23, pp. 359-367, April 2021

Research Article

Different Adaptive Modified Riesz Mean Filter For High-Density Salt-and-Pepper Noise Removal in Grayscale Images

Samet Memiş[1*], Uğur Erkan[2]

[1] Çanakkale Onsekiz Mart University, Faculty of Arts and Sciences, Department of Mathematics, Çanakkale, Turkey, (ORCID: 0000-0002-0958-5872), samettmemis@gmail.com

[2] Karamanoğlu Mehmetbey University, Faculty of Engineering, Department of Computer Engineering, Karaman, Turkey, (ORCID: 0000-0002-2481-0230), uerkan80@gmail.com

(First received 2 February 2021 and in final form 4 April 2021)

(**DOI:** 10.31590/ejosat.873312)

ATIF/REFERENCE: Memiş, S., & Erkan, U., (2021). Different Adaptive Modified Riesz Mean Filter For High-Density Salt-and-Pepper Noise Removal in Grayscale Images. *European Journal of Science and Technology*, (23), 359-367.

Abstract

This paper proposes a new filter, Different Adaptive Modified Riesz Mean Filter (DAMRmF), for high-density salt-and-pepper noise (SPN) removal. DAMRmF operationalizes a pixel weight function and adaptivity condition of Adaptive Median Filter (AMF). In the simulation, the proposed filter is compared with Adaptive Frequency Median Filter (AFMF), Three-Values-Weighted Method (TVWM), Unbiased Weighted Mean Filter (UWMF), Different Applied Median Filter (DAMF), Adaptive Weighted Mean Filter (AWMF), Adaptive Cesáro Mean Filter (ACmF), Adaptive Riesz Mean Filter (ARmF), and Improved Adaptive Weighted Mean Filter (IAWMF) for 20 traditional test images with noise levels from 60% to 90%. The results show that DAMRmF outperforms the state-of-the-art filters in terms of Peak Signal-to-Noise Ratio (PSNR) and Structural Similarity (SSIM) values. Moreover, DAMRmF also performs better than the state-of-the-art filters concerning mean PSNR and SSIM results. We finally discuss DAMRmF for further research.

Keywords: Salt-and-pepper noise, Non-linear functions, Noise removal, Matrix algebra, Image denoising, Riesz mean.

Gri Tonlamalı Görüntülerdeki Yüksek Yoğunluklu Tuz ve Biber Gürültüsünü Kaldırmak için Farklı Uyarlamalı Modifiye Riesz Ortalama Filtresi

Öz

Bu makale, yüksek yoğunluklu tuz ve biber gürültüsünün (SPN) giderilmesi için yeni bir Farklı Uyarlamalı Modifiye Riesz Ortalama Filtresi (DAMRmF) önermektedir. DAMRmF, bir piksel ağırlık fonksiyonu ve Uyarlamalı Medyan Filtresinin (AMF) uyarlanabilirlik koşulunu çalıştırır. Deneysel çalışmada önerilen filtre, %60 ve %90 kadar çeşitli gürültü yoğunluklarındaki 20 geleneksel test görüntüsü için Uyarlanabilir Frekans Medyan Filtresi (AFMF), Üç Değerli Ağırlıklı Yöntem (TVWM), Tarafsız Ağırlıklı Ortalama Filtresi (UWMF), Farklı Uygulanan Medyan Filtresi (DAMF), Uyarlamalı Ağırlıklı Ortalama Filtresi (AWMF), Uyarlamalı Cesáro Ortalama Filtresi (ACmF), Uyarlamalı Riesz Ortalama Filtresi (ARmF) ve Geliştirilmiş Uyarlamalı Ağırlıklı Ortalama Filtresi (IAWMF) karşılaştırılır. Sonuçlar, DAMRmF'nin Tepe Sinyal-Gürültü Oranı (PSNR) ve Yapısal Benzerlik (SSIM) değerleri açısından son teknoloji filtrelerden daha iyi performans sergilediğini göstermektedir. Ayrıca, ortalama PSNR ve SSIM sonuçlarına göre de DAMRmF son teknoloji filtrelerden daha iyi bir performansa sahiptir. Son olarak, gelecek çalışmalar için DAMRmF'yi tartışıyoruz.

Anahtar Kelimeler: Tuz ve biber gürültüsü, Lineer olmayan fonksiyonlar, Gürültü kaldırma, Matris cebiri, Gürültü giderme, Riesz ortalama.

[*] Corresponding Author: samettmemis@gmail.com

1. Introduction

A great variety of the images such as medical images (Öziç & Özşen, 2020), astronomical images (Hausen & Robertson, 2020), and satellite images (Zeren et al., 2020) can be acquired thanks to the development of technology. During the acquisition and transfer of these images, some corruption called noise may occur (Erkan & Gökrem, 2018). There are various noise types such as additive noise, Gaussian noise, impulse noise, and speckle noise affecting the images' quality. Random valued impulse noise (RVIN) and fixed valued impulse noise (or salt-and-pepper noise) (SPN) are two types of impulse noise. RVIN replaces the images' pixels with a random pixel value, while SPN does with a minimum or maximum pixel value (Gonzalez & Woods, 2018). The minimum and maximum pixel values are 0 and 255 for an 8-bit greyscale image, respectively. SPN results from reasons such as sensors, electrical conditions, and transmission errors. The SPN is observed as white (255) and black (0) dots in the images. Therefore, the term "Salt-and-pepper noise" comes from there.

Recently, various approaches have been proposed to remove SPN. Standard Median Filter (SMF) (Tukey, 1977; Pratt, 1975) and Adaptive Median Filter (Hwang & Haddad, 1995) are pioneer approaches and commonly employed for SPN removal. SMF utilizes fixed window size (3×3, 5×5, and 7×7, etc.) and is applied to all pixels. Unlike SMF, AMF using adaptive window size determines the pixels as noisy or noise-free and is implemented to only noisy pixels. Adaptive Weighted Mean Filter (AWMF) (Zhang & Li, 2014) and Unbiased Weighted Mean Filter (UWMF) (Kandemir et al., 2015) are designed to remove high-density SPN. AWMF firstly specifies the adaptive window size by constantly augmenting the window size till consecutive windows' maximum and minimum values are equal. If the considered pixel equals the maximum or minimum values, it may be a noisy pixel. If not, it is regarded as a noise-free pixel. Afterwards, possible noisy pixel replaces with the weighted mean of noise-free pixels. Here, it must be noted that the weighted mean accepts the weight of noisy pixels as 0 and those of the noise-free pixels as 1. UWMF has three phases for image denoising: It determines noisy pixels, recalibrates the pixel weights, and likely noisy pixel is replaced by recalibrated weighted mean.

One of the other image denoising filters implementing weighted mean is Three-Values-Weighted Method (TVWM) (Lu et al., 2016). In the first phase, it uses a variable-size local window to analyze all extreme pixels. TVWM then classifies non-extreme pixels and locates them in the maximum, middle, or minimum groups. Using the weights obtained from distribution ratios of these groups, non-extreme pixels are weighted. The noisy pixel in the centre of the window is restored by employing these weighted values.

Different Applied Median Filter (DAMF) (Erkan et al. 2018) is one of the state-of-the-art SPN filters. It bases on the median function and an adaptive window according to whether all pixels in the considered window are zero or not. Thus, it outperforms many filters at low-density, middle-density, and high-density SPN. AWMF performs better than DAMF at high-density SPN while DAMF does not achieve. DAMF's this deficiency has been eliminated by operationalizing Cesáro mean (arithmetic mean) instead of median and increasing adaptive windows, and Adaptive Cesáro Mean Filter (ACmF) (Enginoğlu et al., 2020) has been suggested. ACmF accepts the weights of the noisy-free pixels as 1. To consider the weights of the noise-free pixels concerning the centre pixel in the window, a pixel similarity-based Adaptive Riesz Mean Filter (ARmF) (Enginoğlu et al., 2019) has been introduced. ARmF avails of the pixel similarity that calculates the similarity between the considered pixel and centre pixel in the window. If the pixels' locations are close to each other, it produces a value close to 1. ARmF, firstly, constructs a binary matrix detecting the noisy pixels. It then produces a new pixel value for each noisy pixel thanks to the pixel similarity of noise-free pixels to the centre and adaptive windowing concerning whether the window is equal to a zero matrix or not. In this way, ARmF achieves better Peak Signal-to-Noise Ratio (PSNR) and Structural Similarity (SSIM) (Wang et al., 2004) results than SMF, AMF, AWMF, and DAMF. Combining this filtering success of ARmF with the windowing advantage of AWMF, a novel high-density-SPN filter, namely Improved Adaptive Weighted Mean Filter (IAWMF) (Erkan et al., 2020b), has been offered. As distinct from ARmF, IAWMF employs Euclidean pixel similarity to weight the noise-free pixels. Integrating this weighting process into AWMF, IAWMF outperforms AWMF, DAMF, and ARMF at any noise densities. Utilizing a new median named frequency median, an Adaptive Frequency Median Filter (AFMF) (Erkan et al., 2020a), an improved version of AMF, has been developed. AFMF produces better PSNR and SSIM rates than SMF, AMF, and DAMF developed through standard median function.

In this study, we aim to avail of the adaptivity condition of AMF and pixel similarity of ARmF. We develop a high-density SPN filter, i.e., Different Adaptive Modified Riesz Mean Filter (DAMRmF). DAMRmF generates better PSNR and SSIM values than AFMF, TVWM, UWMF, DAMF, AWMF, ACmF, ARmF, and IAWMF at noise levels ranging from 60% to 90% for 20 traditional test images (Weber, 1997).

The rest of the paper is organized as follows: In Section 2, the basic definitions and notations needed in the following sections are presented. In Section 3, a novel SPN filter, DAMRmF, is proposed. In Section 4, an experimental study is carried out to demonstrate the proposed filter outperforms the state-of-the-art filters. Finally, the discussions and concluding remarks related to DAMRmF are provided for further research.

2. Basic Definitions and Notations

Definition 2.1 Let $A \coloneqq [a_{ij}]_{m\times n}$ be an image matrix (IM) such that a_{ij} is an unsigned integer number and $0 \le a_{ij} \le 255$. Then, a_{ij} is called a noisy entry of A if $a_{ij} = 0$ or $a_{ij} = 255$; otherwise, a_{ij} is called a regular entry of A.

Definition 2.2 Let A be an IM. Then, A is called a noise image matrix (NIM) if for some i and j, a_{ij} is a noisy entry of A.

Definition 2.3 Let $A \coloneqq [a_{ij}]_{m\times n}$ and $t \in \{1,2,\dots,\min\{m,n\}\}$. Then, the matrix $[\bar{\bar{a}}_{rs}]_{(m+2t)\times(n+2t)}$ called t-symmetric pad matrix of A is denoted by $\bar{\bar{A}}_{t-sym}$ (or briefly $\bar{\bar{A}}_t$) and is defined as follows:

$$\begin{bmatrix} a_{tt} & \cdots & a_{t1} & a_{t1} & a_{t2} & \cdots & a_{tn} & a_{tn} & \cdots & a_{t(n-t+1)} \\ \vdots & \ddots & \vdots & \vdots & \vdots & \ddots & \vdots & \vdots & \ddots & \vdots \\ a_{1t} & \cdots & a_{11} & a_{11} & a_{12} & \cdots & a_{1n} & a_{1n} & \cdots & a_{1(n-t+1)} \\ a_{1t} & \cdots & a_{11} & \boldsymbol{a_{11}} & \boldsymbol{a_{12}} & \cdots & \boldsymbol{a_{1n}} & a_{1n} & \cdots & a_{1(n-t+1)} \\ a_{2t} & \cdots & a_{21} & \boldsymbol{a_{21}} & \boldsymbol{a_{22}} & \cdots & \boldsymbol{a_{2n}} & a_{2n} & \cdots & a_{2(n-t+1)} \\ a_{3t} & \cdots & a_{31} & \boldsymbol{a_{31}} & \boldsymbol{a_{32}} & \cdots & \boldsymbol{a_{3n}} & a_{3n} & \cdots & a_{3(n-t+1)} \\ \vdots & \ddots & \vdots & \vdots & \vdots & \ddots & \vdots & \vdots & \ddots & \vdots \\ a_{mt} & \cdots & a_{m1} & \boldsymbol{a_{m1}} & \boldsymbol{a_{m2}} & \cdots & \boldsymbol{a_{mn}} & a_{mn} & \cdots & a_{m(n-t+1)} \\ a_{mt} & \cdots & a_{m1} & a_{m1} & a_{m2} & \cdots & a_{mn} & a_{mn} & \cdots & a_{m(n-t+1)} \\ \vdots & \ddots & \vdots & \vdots & \vdots & \ddots & \vdots & \vdots & \ddots & \vdots \\ a_{(m-t+1)t} & \cdots & a_{(m-t+1)1} & a_{(m-t+1)1} & a_{(m-t+1)2} & \cdots & a_{(m-t+1)n} & a_{(m-t+1)n} & \cdots & a_{(m-t+1)(n-t+1)} \end{bmatrix} \quad (1)$$

Definition 2.4 Let A be an NIM. Then, the matrix $B \coloneqq [b_{ij}]_{m\times n}$ is called a binary matrix of A where

$$b_{ij} = \begin{cases} 0, & a_{ij} \text{ is a noisy entry of } A \\ 1, & \text{otherwise} \end{cases} \quad (2)$$

Example 2.1 Let $A \coloneqq \begin{bmatrix} 255 & 87 & 89 \\ 45 & 255 & 0 \\ 100 & 22 & 63 \end{bmatrix}$. Then,

$$\bar{\bar{A}}_2 = \begin{bmatrix} 255 & 45 & 45 & 255 & 0 & 0 & 255 \\ 87 & 255 & 255 & 87 & 89 & 89 & 87 \\ 87 & 255 & \mathbf{255} & \mathbf{87} & \mathbf{89} & 89 & 87 \\ 255 & 45 & \mathbf{45} & \mathbf{255} & \mathbf{0} & 0 & 255 \\ 22 & 100 & \mathbf{100} & \mathbf{22} & \mathbf{63} & 63 & 22 \\ 22 & 100 & 100 & 22 & 63 & 63 & 22 \\ 255 & 45 & 45 & 255 & 0 & 0 & 255 \end{bmatrix}_{7\times 7}$$

Definition 2.5 Let $A \coloneqq [a_{ij}]_{m\times n}$ and $k \in \{1,2,\dots,\mathrm{t}\}$. Then, the matrix

$$\begin{bmatrix} \bar{\bar{a}}_{(i+t-k)(j+t-k)} & \cdots & \bar{\bar{a}}_{(i+t-k)(j+t+k)} \\ \vdots & \bar{\bar{a}}_{(i+t)(j+t)} & \vdots \\ \bar{\bar{a}}_{(i+t+k)(j+t-k)} & \cdots & \bar{\bar{a}}_{(i+t+k)(j+t+k)} \end{bmatrix}_{(2k+1)\times(2k+1)} \quad (3)$$

is called k-approximate matrix of a_{ij} in $\bar{\bar{A}}_t$ and is denoted by A_{ij}^k.

Example 2.2 Let's consider Example 2.1. Then,

$$A_{32}^1 = \begin{bmatrix} \bar{\bar{a}}_{43} & \bar{\bar{a}}_{44} & \bar{\bar{a}}_{45} \\ \bar{\bar{a}}_{53} & \bar{\bar{a}}_{54} & \bar{\bar{a}}_{55} \\ \bar{\bar{a}}_{63} & \bar{\bar{a}}_{64} & \bar{\bar{a}}_{65} \end{bmatrix} = \begin{bmatrix} 45 & 255 & 0 \\ 100 & 22 & 63 \\ 100 & 22 & 63 \end{bmatrix}.$$

Definition 2.6 A matrix with all its entries being zero is called a zero or null matrix and is denoted by $[0]$.

Definition 2.7 Let $A \coloneqq [a_{ij}]_{m\times n}$. The matrix $\tilde{A} \coloneqq [\tilde{a}_{1u}]_{1\times(m.n)}$ consists of all entries (elements) of A and being non-decreasing is called an entry matrix (EM) of A.

Example 2.3 Let us consider Example 2.2. Then, $\tilde{A}_{32}^1 = [0 \quad 22 \quad 22 \quad 45 \quad 63 \quad 63 \quad 100 \quad 100 \quad 255]$.

Definition 2.8 Let $\tilde{A} \coloneqq [\tilde{a}_{1u}]_{1\times(m.n)}$ be an EM of $A \coloneqq [a_{ij}]_{m\times n}$. The value

$$\mathrm{med}(\tilde{A}) \coloneqq \begin{cases} \tilde{a}_{1\left(\frac{m.n+1}{2}\right)}, & \frac{m.n+1}{2} \in \mathbb{Z} \\ \frac{1}{2}\left(\tilde{a}_{1\left(\frac{m.n}{2}\right)} + \tilde{a}_{1\left(\frac{m.n+2}{2}\right)}\right), & \frac{m.n}{2} \in \mathbb{Z} \end{cases} \quad (4)$$

is called a median of $\tilde{A}$.

Definition 2.9 Let A be an IM. Then, the value

$$\mathrm{ps}(a_{ij}, a_{st}) \coloneqq \left(\frac{1}{1+|i-s|+|j-t|}\right)^2$$

is called pixel similarity between a_{ij} and a_{st}

Definition 2.10 Let A be an NIM. Then the value

$$\mathrm{Rm}(A_{ij}^k) \coloneqq \frac{\sum_{(s,t)\in I_{ij}^k} \mathrm{ps}(a_{st}, a_{(k+1)(k+1)})a_{st}}{\sum_{(s,t)\in I_{ij}^k} \mathrm{ps}(a_{st}, a_{(k+1)(k+1)})} \quad (5)$$

is called Riesz mean of A_{ij}^k.

Here, $I_{ij}^k \coloneqq \{(s,t):\ a_{st} \textit{ is a regular entry of } A_{ij}^k\}$

3. Proposed Salt-and-Pepper Filter

In this section, firstly, we present pseudo-codes of AMF (Hwang & Haddad, 1995) (Algorithm 1) and ARmF (Enginoğlu et al., 2019) (Algorithm 2). AMF operates median filter and median-based adaptivity condition to remove SPN. ARmF utilizes pixel similarity-based Riesz mean of the considered window. Besides, it employs an adaptivity condition that relies on whether the k-approximate matrix equals a zero matrix or not.

Algorithm 1.
Adaptive Median Filter (AMF)

Input: NIM $A \coloneqq [a_{ij}]_{m\times n}$
Output: Denoised $A \coloneqq [a_{ij}]_{m\times n}$
Initialize $k_{max} = 9$
Compute $\bar{\bar{A}}_{k_{max}}$
For all i and j
  For k from 1 to k_{max}
    If $\left(\min(\bar{A}_{ij}^k) < \mathrm{med}(\bar{A}_{ij}^k)$ **AND** $\mathrm{med}(\bar{A}_{ij}^k) < \max(\bar{A}_{ij}^k)\right)$ **AND** $\left(a_{ij} = \min(\bar{A}_{ij}^k)$ **OR** $a_{ij} = \max(\bar{A}_{ij}^k)\right)$
      $a_{ij} \leftarrow \mathrm{med}(\tilde{A}_{ij}^k)$
      Break
    End If
  End For
End For

Algorithm 2.
Adaptive Riesz Mean Filter (ARmF)

Input: NIM $A \coloneqq [a_{ij}]_{m\times n}$ such that $\min\{m,n\} \geq 5$
Output: Denoised $A \coloneqq [a_{ij}]_{m\times n}$
Convert A from uint8 form to double form
For t from 5 to 1
  Compute the binary matrix $B \coloneqq [b_{ij}]_{m\times n}$ of A
  Compute $\bar{\bar{A}}_t$ and $\bar{\bar{B}}_t$
  For all i and j
    If $b_{ij} = 0$
      For k from 1 to t
        If $B_{ij}^k \neq [0]$
          $a_{ij} \leftarrow \mathrm{Rm}(A_{ij}^k)$
          Break
        End If
      End For
    End If
  End For
End For

Secondly, we define modified Riesz mean (MRm) and propose Different Adaptive Modified Riesz Mean Filter (DAMRmF) employing MRm and adaptivity condition of AMF. DAMRmF removes SPN operationalizing the weight of the considered pixel according to the centre pixel in the window. DAMRmF is designed to be outperformed at high-density SPN.

Definition 2.11 Let A be an NIM. Then the value

$$\mathrm{MRm}(A_{ij}^k) \coloneqq \frac{\sum_{(s,t)\in I_{ij}^k} \mathrm{pw}(a_{st}, k)a_{st}}{\sum_{(s,t)\in I_{ij}^k} \mathrm{pw}(a_{st}, k)} \quad (6)$$

is called Modified Riesz mean of A_{ij}^k. Here, $\mathrm{pw}(a_{st}, k) \coloneqq \left(\frac{1}{1+(k+1-s)^2+(k+1-t)^2}\right)^2$ and $I_{ij}^k \coloneqq \{(s,t):\ a_{st} \text{ is a regular entry of } A_{ij}^k\}$ stand for the pixel weight of a_{st} in A_{ij}^k and the set of all indexes of the regular pixels in A_{ij}^k, respectively.

The pixel weight function to be employed with the adaptivity condition simultaneously is defined to deal with high-density SPN. It produces different weights and these weights more efficacious than those of pixel similarity in ARmF. Thus, DARmF using the pixel weight performs better than the state-of-the-art filters in high-density SPN for 20 traditional greyscale images.

Finally, we provide the pseudo-code of DAMRmF in Algorithm 3 and its flowchart in Figure 1.

Algorithm 3.
Different Adaptive Modified Riesz Mean Filter (DAMRmF)

Input: Read an NIM $A \coloneqq [a_{ij}]_{m\times n}$ such that $\min\{m,n\} \geq 5$
Output: Denoised $A \coloneqq [a_{ij}]_{m\times n}$
Convert A from uint8 form to double form
For t from 5 to 1
  Compute the binary matrix $B \coloneqq [b_{ij}]_{m\times n}$ of A
  Compute $\bar{\bar{A}}_t$ and $\bar{\bar{B}}_t$
  For all i and j
    If $b_{ij} = 0$
      For k from 1 to t
        If $\left(0 < \text{med}(\tilde{A}_{ij}^k)\right.$ **AND** $\left.\text{med}(\tilde{A}_{ij}^k) < 255\right)$ **AND** $(a_{ij} = 0$ **OR** $a_{ij} = 255)$
          $a_{ij} \leftarrow \text{MRm}(A_{ij}^k)$
          Break
        End If
      End For
    End If
  End For
End For

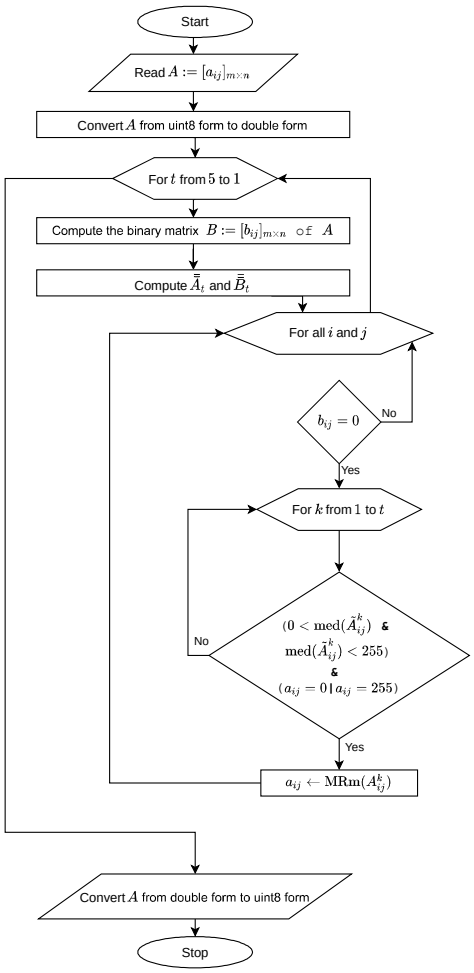

Figure 1. The flowchart of DAMRmF

4. Experimental Study

In this part of the study, we compare the proposed DAMRmF with AFMF (Erkan et al., 2020a), TVWA (Lu et al., 2016), UWMF (Kandemir et al., 2015), DAMF (Erkan et al., 2018), AWMF (Zang & Li, 2014), ACmF (Enginoğlu et al., 2020), ARmF (Enginoğlu et al., 2019), and IAWMF (Erkan et al., 2020b) in terms of PSNR and SSIM (Wang et al., 2004) results.

4.1. Image Quality Assessment Metrics

In this subsection, we present the mathematical notations of PSNR and SSIM. Let $X \coloneqq [x_{ij}]$ and $Y \coloneqq [y_{ij}]$ be the original image and restored image, respectively.

PSNR is defined by

$$\text{PSNR}(X,Y) \coloneqq 10\log\left(\frac{255^2}{\text{MSE}(X,Y)}\right) \tag{7}$$

where $\text{MSE}(X,Y)$ represents the Mean Square Error, and it is defined by

$$\text{MSE}(X,Y) \coloneqq \frac{1}{mn}\sum_{i=1}^{m}\sum_{j=1}^{n}(x_{ij}-y_{ij})^2 \tag{8}$$

SSIM is defined by

$$\text{SSIM}(X,Y) \coloneqq \frac{(2\mu_X\mu_Y + C_1) + (2\sigma_{XY} + C_2)}{(\mu_X^2 + \mu_Y^2 + C_1) + (\sigma_X^2 + \sigma_Y^2 + C_2)} \tag{10}$$

where μ_X, μ_Y, σ_X, σ_Y, and σ_{XY} are the average intensities, standard deviations, and cross-covariance of images X and Y, respectively. Additionally, $C_1 \coloneqq (K_1L)^2$ and $C_2 \coloneqq (K_2L)^2$ are two constants such that $K_1 = 0.01$, $K_2 = 0.03$ and $L = 255$ for 8-bit grayscale images.

4.2. Simulation Results

In this subsection, we simulate DAMRmF, AFMF, TVWA, UWMF, DAMF, AWMF, ACmF, ARmF, and IAWMF using 20 traditional test images (Weber, 1997) with 512×512 (Lena, Cameraman, Barbara, Baboon, Peppers, Living Room, Lake, Plane, Hill, Pirate, Boat, House, Bridge, Elaine, Flintstones, Flower, Parrot, Dark-Haired Woman, Blonde Woman, and Einstein). We carry out the simulations by utilizing MATLAB R2020b and a laptop with I(R) Core(TM) CPU i5-4200H@2.8GHz and 8 GB RAM.

Table 1 presents the mean PSNR results of the filters for 20 traditional images with high-density SPN. The results show that DAMRmF performs better than the others in considered SPN ratios.

Table 1. Mean PSNR results for 20 traditional images with different SPN ratios ranging from 60% *to* 90%

Filters	60%	65%	70%	75%	80%	85%	90%	Mean
AFMF	28.15	27.38	26.44	25.45	24.21	22.74	20.64	25.00
TVWA	30.09	29.38	28.62	27.79	26.73	24.46	19.01	26.58
UWMF	30.00	29.31	28.67	27.92	27.07	26.22	25.08	27.75
DAMF	29.74	29.07	28.38	27.62	26.76	25.80	24.43	27.40
AWMF	30.25	29.54	28.79	27.97	27.07	26.06	24.74	27.77
ACmF	30.36	29.61	28.83	27.99	27.08	26.07	24.75	27.81
ARmF	30.57	29.79	28.97	28.10	27.16	26.12	24.78	27.93
IAWMF	30.73	30.02	29.27	28.46	27.55	26.56	25.29	28.27
DAMRmF	**30.74**	**30.04**	**29.32**	**28.50**	**27.64**	**26.68**	**25.41**	**28.33**

Secondly, Table 2 offers the mean SSIM results of the filters for 20 traditional images with high-density SPN. The results manifest that DAMRmF outperforms the others in considered SPN ratios.

Thirdly, Table 3 and 4 are related to PSNR and SSIM results for several test images with various high SPN ratios, respectively. DAMRmF exhibits maximum performance concerning PSNR and SSIM values. Moreover, DAMRmF outperforms IAWMF being efficacious for high-density SPN.

Fourthly, Figure 2 offers the visual results of the methods concerning denoising of the "Lena" image with an SPN ratio of 90%. Moreover, Figure 3 presents the visual results of denoising of the proposed method for "Pepper" image with SPN ratios of 60%, 70%, 80%, and 90%. Although AFMF removes the noise to a great extent, the denoised image has blurring details, and AFMF has not preserved the edges in "Lena" image. The image denoised by TVWM has black speckle exceedingly as well as it has blurring details. Denoising results of DAMRmF and the others efficacious. Moreover, DAMRmF has smooth details and display a better visual quality than the others.

Fifthly, the PSNR and SSIM graphs are provided in Figure 4 and 5 concerning "House", "Elaine", "Blonde Woman", and "Lake" images, respectively.

Table 2. Mean SSIM results for 20 traditional images with different SPN ratios ranging from 60% *to* 90%

Filters	60%	65%	70%	75%	80%	85%	90%	Mean
AFMF	0.8461	0.8259	0.8007	0.7694	0.7296	0.6784	0.6039	0.7506
TVWA	0.8882	0.8710	0.8511	0.8271	0.7972	0.7410	0.5671	0.7918
UWMF	0.8855	0.8687	0.8499	0.8278	0.8016	0.7696	0.7245	0.8182
DAMF	0.8804	0.8635	0.8438	0.8204	0.7926	0.7573	0.7045	0.8089
AWMF	0.8871	0.8703	0.8506	0.8267	0.7985	0.7629	0.7113	0.8153
ACmF	0.8893	0.8719	0.8518	0.8276	0.7991	0.7632	0.7115	0.8163
ARmF	0.8929	0.8756	0.8554	0.8311	0.8023	0.7660	0.7139	0.8196
IAWMF	0.8952	0.8794	0.8612	0.8390	0.8126	0.7791	0.7317	0.8283
DAMRmF	**0.8959**	**0.8802**	**0.8621**	**0.8400**	**0.8142**	**0.7816**	**0.7348**	**0.8298**

Table 3. PSNR results of the filters for several traditional images with different SPN ratios ranging from 60% *to* 90%

Images	Filters	60%	65%	70%	75%	80%	85%	90%	Mean
Lena	AFMF	30.03	29.09	28.11	27.24	25.92	24.29	22.02	26.67
	TVWA	32.27	31.47	30.49	29.71	28.48	25.87	19.52	28.26
	UWMF	32.09	31.26	30.40	29.74	28.83	27.89	26.60	29.54
	DAMF	31.75	31.04	30.17	29.44	28.49	27.50	26.02	29.20
	AWMF	32.19	31.41	30.48	29.72	28.75	27.76	26.29	29.51
	ACmF	32.30	31.48	30.52	29.74	28.76	27.76	26.29	29.55
	ARmF	32.52	31.67	30.63	29.83	28.85	27.82	26.32	29.66
	IAWMF	32.69	31.87	30.98	30.23	29.28	28.25	26.85	30.02
	DAMRmF	**32.72**	**31.91**	**31.03**	**30.29**	**29.37**	**28.34**	**26.95**	**30.09**
Pepper	AFMF	29.20	28.61	27.74	26.46	24.98	23.16	20.69	25.83
	TVWA	31.73	30.99	30.25	29.54	28.24	26.15	20.02	28.13
	UWMF	31.31	30.67	30.06	29.44	28.40	27.66	26.51	29.15
	DAMF	31.13	30.53	29.89	29.17	28.07	27.24	25.85	28.84
	AWMF	31.71	30.96	30.28	29.53	28.36	27.46	26.13	29.20
	ACmF	31.78	31.02	30.30	29.54	28.36	27.46	26.14	29.23
	ARmF	31.85	31.09	30.35	29.60	28.39	27.49	26.16	29.28
	IAWMF	31.94	31.28	30.65	29.96	28.82	27.96	26.71	29.62
	DAMRmF	**32.13**	**31.46**	**30.82**	**30.11**	**28.94**	**28.13**	**26.86**	**29.78**
Lake	AFMF	26.60	25.83	24.68	23.61	22.30	20.99	18.91	23.27
	TVWA	28.85	28.13	27.22	26.39	25.44	23.74	18.40	25.45
	UWMF	28.77	28.10	27.29	26.52	25.63	24.77	23.55	26.38
	DAMF	28.36	27.69	26.86	26.06	25.21	24.30	22.89	25.91
	AWMF	28.78	28.10	27.21	26.36	25.47	24.54	23.11	26.22
	ACmF	28.92	28.19	27.27	26.39	25.49	24.54	23.11	26.28
	ARmF	29.13	28.36	27.42	26.51	25.58	24.61	23.16	26.40
	IAWMF	29.28	28.60	27.73	26.91	25.99	25.05	23.71	26.75
	DAMRmF	**29.33**	**28.68**	**27.80**	**26.97**	**26.05**	**25.16**	**23.83**	**26.83**
Dark-Haired Woman	AFMF	35.69	34.54	33.05	31.77	30.09	27.48	24.53	31.02
	TVWA	38.28	37.38	36.65	35.23	33.70	28.53	20.47	32.89
	UWMF	38.07	37.19	36.60	35.56	34.68	33.37	32.20	35.38
	DAMF	37.56	36.81	36.14	35.12	34.19	32.72	31.08	34.80
	AWMF	38.27	37.36	36.64	35.54	34.60	33.07	31.74	35.32
	ACmF	38.35	37.44	36.68	35.57	34.61	33.07	31.74	35.35
	ARmF	38.55	37.60	36.80	35.67	34.69	33.14	31.78	35.46
	IAWMF	38.81	37.93	37.21	36.14	35.21	33.71	32.46	35.92
	DAMRmF	**38.99**	**38.08**	**37.41**	**36.30**	**35.41**	**33.91**	**32.61**	**36.10**

Table 4. SSIM results of the filters for several traditional images with different SPN ratios ranging from 60% *to* 90%

Images	Filters	60%	65%	70%	75%	80%	85%	90%	Mean
Lena	AFMF	0.8857	0.8706	0.8526	0.8285	0.8007	0.7592	0.6946	0.8131
	TVWA	0.9140	0.9005	0.8837	0.8647	0.8392	0.7875	0.5970	0.8267
	UWMF	0.9108	0.8972	0.8813	0.8645	0.8443	0.8185	0.7812	0.8568
	DAMF	0.9079	0.8949	0.8784	0.8594	0.8375	0.8100	0.7663	0.8506
	AWMF	0.9131	0.8999	0.8835	0.8646	0.8426	0.8156	0.7731	0.8561
	ACmF	0.9144	0.9009	0.8841	0.8650	0.8429	0.8156	0.7731	0.8566
	ARmF	0.9173	0.9038	0.8866	0.8674	0.8453	0.8173	0.7745	0.8589
	IAWMF	0.9194	0.9071	0.8921	0.8750	0.8555	0.8295	0.7915	0.8671
	DAMRmF	**0.9205**	**0.9085**	**0.8939**	**0.8771**	**0.8582**	**0.8334**	**0.7951**	**0.8695**
Pepper	AFMF	0.8178	0.8039	0.7864	0.7613	0.7263	0.6827	0.6093	0.7411
	TVWA	0.8627	0.8439	0.8254	0.8037	0.7750	0.7309	0.5785	0.7743
	UWMF	0.8442	0.8268	0.8105	0.7922	0.7688	0.7463	0.7163	0.7864
	DAMF	0.8508	0.8332	0.8151	0.7938	0.7669	0.7396	0.7003	0.7857
	AWMF	0.8630	0.8441	0.8258	0.8034	0.7751	0.7466	0.7078	0.7951
	ACmF	0.8635	0.8445	0.8259	0.8035	0.7752	0.7464	0.7078	0.7952
	ARmF	0.8613	0.8424	0.8240	0.8021	0.7740	0.7458	0.7079	0.7939
	IAWMF	0.8611	0.8445	0.8286	0.8099	0.7851	0.7605	0.7279	0.8025
	DAMRmF	**0.8681**	**0.8522**	**0.8365**	**0.8179**	**0.7935**	**0.7696**	**0.7362**	**0.8106**
Lake	AFMF	0.8353	0.8137	0.7850	0.7491	0.7075	0.6516	0.5746	0.7310
	TVWA	0.8777	0.8596	0.8361	0.8108	0.7800	0.7256	0.5556	0.7779
	UWMF	0.8670	0.8496	0.8287	0.8064	0.7793	0.7470	0.7009	0.7970
	DAMF	0.8698	0.8520	0.8287	0.8039	0.7739	0.7362	0.6816	0.7923
	AWMF	0.8765	0.8587	0.8355	0.8103	0.7800	0.7425	0.6873	0.7987
	ACmF	0.8789	0.8606	0.8369	0.8112	0.7807	0.7429	0.6875	0.7998
	ARmF	0.8801	0.8620	0.8385	0.8130	0.7827	0.7449	0.6899	0.8016
	IAWMF	0.8808	0.8647	0.8437	0.8210	0.7933	0.7589	0.7094	0.8103
	DAMRmF	**0.8840**	**0.8680**	**0.8473**	**0.8240**	**0.7963**	**0.7632**	**0.7135**	**0.8138**
Dark-Haired Woman	AFMF	0.9392	0.9294	0.9164	0.9001	0.8790	0.8435	0.7858	0.8848
	TVWA	0.9567	0.9493	0.9410	0.9291	0.9163	0.8695	0.6797	0.8917
	UWMF	0.9543	0.9469	0.9394	0.9289	0.9193	0.9037	0.8832	0.9251
	DAMF	0.9524	0.9452	0.9367	0.9251	0.9140	0.8955	0.8660	0.9193
	AWMF	0.9566	0.9493	0.9409	0.9293	0.9184	0.8999	0.8741	0.9241
	ACmF	0.9572	0.9499	0.9413	0.9296	0.9186	0.9000	0.8742	0.9244
	ARmF	0.9584	0.9511	0.9425	0.9308	0.9197	0.9010	0.8751	0.9255
	IAWMF	0.9597	0.9533	0.9459	0.9360	0.9266	0.9104	0.8890	0.9315
	DAMRmF	**0.9612**	**0.9548**	**0.9480**	**0.9381**	**0.9296**	**0.9142**	**0.8937**	**0.9342**

Figure 2. Image denoising results of the compared filters with SPN level of 90% of the "Lena" image (512×512 *pixels).*

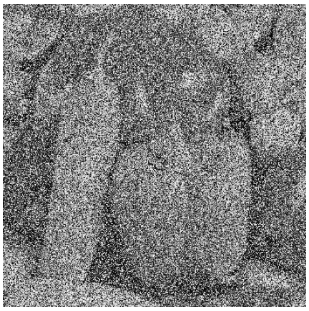

SPN ratio 60%
PSNR/SSIM (7.51/0.0179)

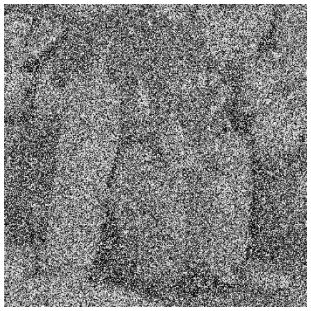

SPN ratio 70%
PSNR/SSIM (6.84/0.133)

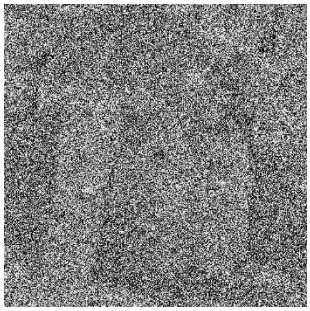

SPN ratio 80%
PSNR/SSIM (6.24/0.0086)

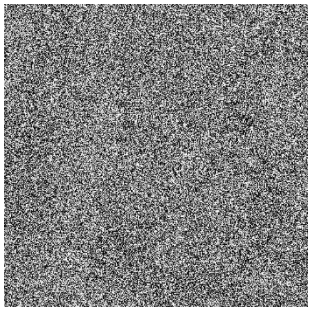

SPN ratio 90%
PSNR/SSIM (5.75/0.0063)

Denoising of SPN
PSNR/SSIM (32.13/0.8681)

Denoising of SPN
PSNR/SSIM (30.82/0.8365)

Denoising of SPN
PSNR/SSIM (28.94/0.7935)

Denoising of SPN
PSNR/SSIM (26.86/0.7362)

Figure 3. Image denoising results of the proposed filter with various SPN levels of the "Pepper" image (512 × 512 pixels).

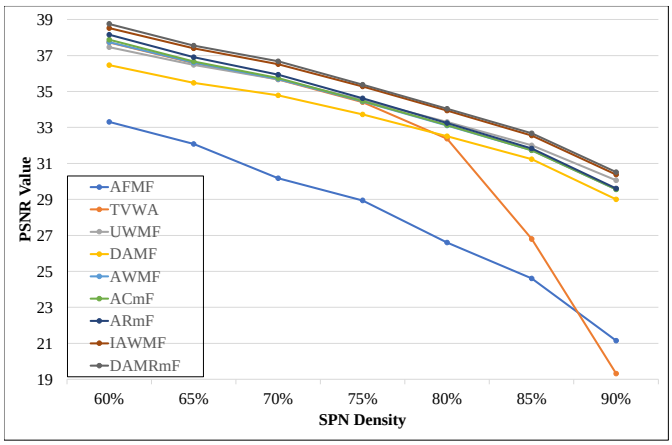

(a)

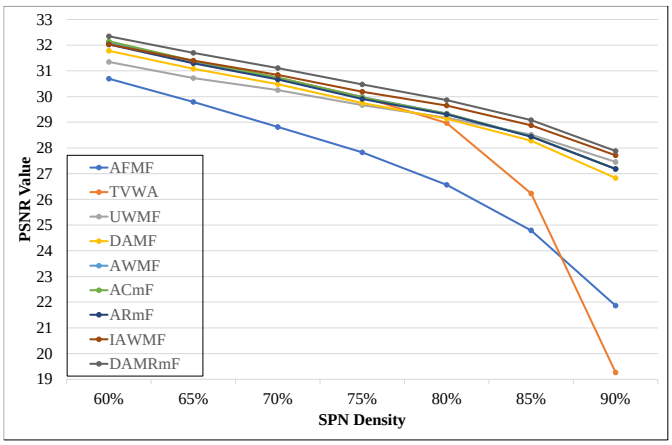

(b)

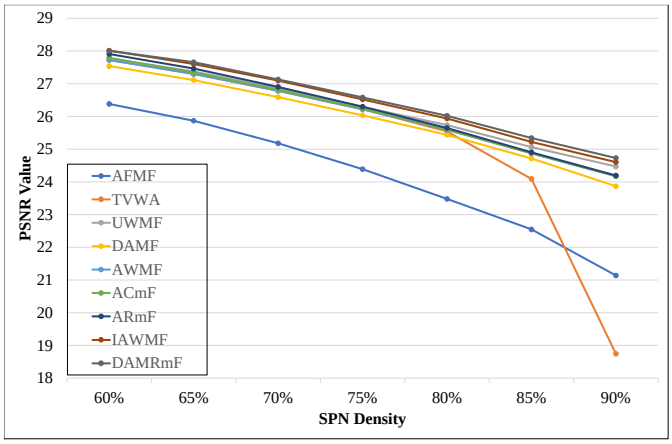

(c)

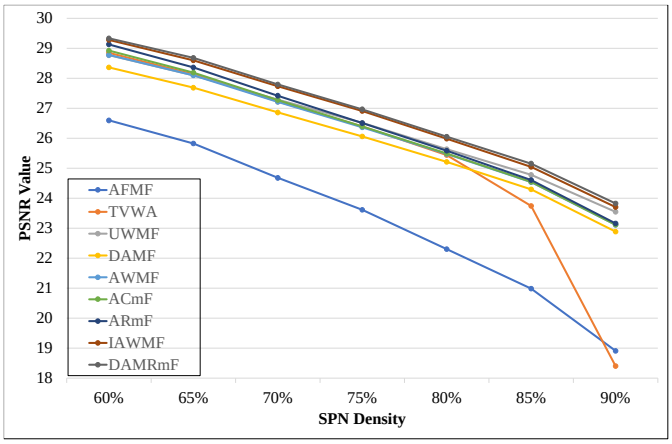

(d)

Figure 4. PSNR Graphs of the several traditional images: (a) House, (b) Elaine, (c) Blonde Woman, and (d) Lake

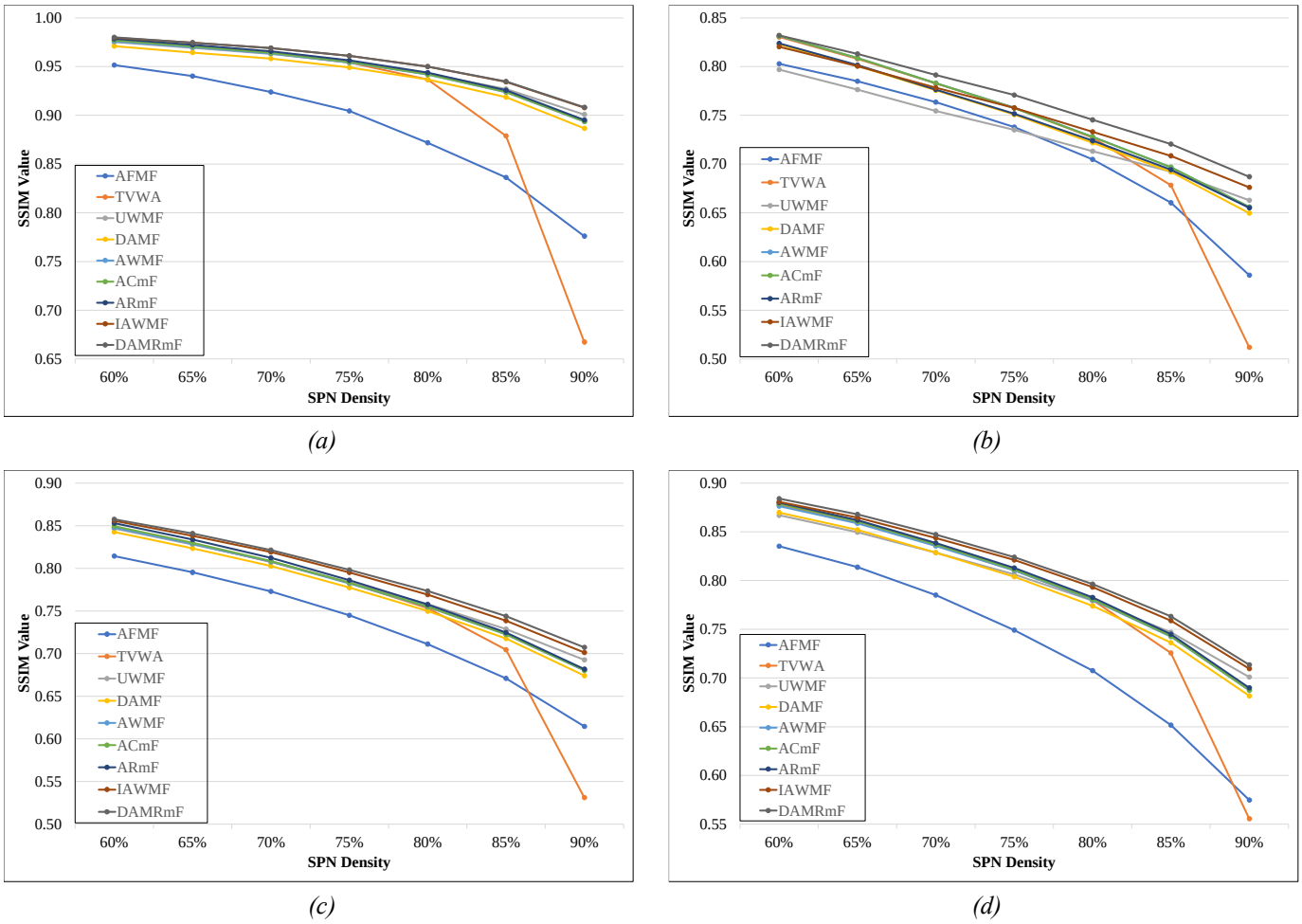

Figure 5. SSIM Graphs of the several traditional images: (a) House, (b) Elaine, (c) Blonde Woman, and (d) Lake

Finally, Table 5 shows the mean running times (seconds) of the methods obtained during the simulations. Even though IAWMF performs better than the other state-of-the-art filters, it operates slower than the others. On the other hand, DAMRmF has an advantage over IAWMF concerning denoising and running time.

Table 5. Mean running time for 20 traditional images with different SPN ratios ranging from 60% to 90% (in second)

Filters	60%	65%	70%	75%	80%	85%	90%	Mean
AFMF	8.82	8.57	8.32	8.08	8.79	7.81	7.49	8.27
TVWA	4.22	4.03	3.88	3.82	3.54	3.28	3.19	3.71
UWMF	1.14	1.16	1.62	1.81	1.64	1.98	2.26	1.66
DAMF	0.84	0.87	0.92	1.01	1.12	1.25	1.40	1.06
AWMF	2.90	2.79	2.80	2.84	2.99	3.19	3.47	3.00
ACmF	1.18	1.23	1.34	1.46	1.62	1.86	2.06	1.54
ARmF	0.66	0.69	0.76	0.82	0.94	1.14	1.24	0.89
IAWMF	10.34	10.60	11.97	12.87	14.76	17.53	22.23	14.33
DAMRmF	3.35	3.82	4.48	5.90	6.50	7.78	10.31	6.02

5. Conclusions and Recommendations

In this study, we defined Modified Riesz Mean replacing the pixel similarity in Riesz mean with pixel weight function. We then employed the Modified Riesz Mean and the adaptivity condition of AMF (Hwang & Haddad, 1995) simultaneously, and developed an efficacious SPN filter, namely DAMRmF, for high-density SPN removal. To indicate the denoising success of the proposed filter, we carried out an experimental study. The simulation results manifest that our DAMRmF outperforms AFMF (Erkan et al., 2020a), TVWA (Lu et al., 2016), UWMF (Kandemir et al., 2015), DAMF (Erkan et al., 2018), AWMF (Zang & Li, 2014), ACmF (Enginoğlu et al., 2020), ARmF (Enginoğlu et al., 2019), and IAWMF (Erkan et al., 2020b) according to PSNR and SSIM (Wang et al., 2004) results for SPN densities varying from 60% to 90%. Besides, visual results herein validated the numerical results provided in the Simulation Results Subsection. Though there is very little difference between PSNR and SSIM values of DAMRmF and IAWMF, DAMRmF runs faster than IAWMF. Therefore, DAMRmF outperforms IAWMF in terms of PSNR value, SSIM value, and running time, and it can be preferred instead of IAWMF. In the experimental study, due to widely using and knowing of the PSNR quality metric, we utilized this quality metric even though it may not generate reliable results.

Although DAMRmF produces better denoising results in high-density SPN removal than the others, it can be improved more through new adaptivity condition or pixel weight. On the other hand, this improvement can be achieved too by including the noise density of the image in the denoising process. Therefore, further research should be focused the defining a new pixel weight function or adaptivity condition.

6. Acknowledgement

The authors would like to thank the editors and reviewers who have contributed to improving this paper.

References

Enginoğlu, S., Erkan, U., & Memiş, S., (2019). Pixel similarity-based adaptive Riesz mean filter for salt-and-pepper noise removal, *Multimedia Tools and Applications, 78*(24), 35401–35418.

Enginoğlu, S., Erkan, U., & Memiş, S., (2020). Adaptive Cesáro mean filter for salt-and-pepper noise removal, El-Cezeri Journal of Science and Engineering, 7(1), 304–314.

Erkan, U., Enginoğlu, S., Thanh, D. N. H., & Hieu, L. M., (2020a). Adaptive frequency median filter for the salt-and-pepper denoising problem, IET Image Processing, 14(7), 1291–1302.

Erkan, U., & Gökrem, L., (2018). A new method based on pixel density in salt and pepper noise removal, *Turkish Journal of Electrical Engineering & Computer Sciences, 26*(1), 162–171.

Erkan, U., Gökrem, L., & Enginoğlu, S., (2018). Different applied median filter in salt and pepper noise, *Computer and Electrical Engineering, 70*, 789–798.

Erkan, U., Thanh, D. N. H., Enginoğlu, S., & Memiş, S., (2020b). Improved adaptive weighted mean filter for salt-and-pepper noise removal, *2020 International Conference on Electrical, Communication, and Computer Engineering (ICECCE)*, Istanbul, Turkey, pp. 1–5.

Gonzalez, R. C., & Woods, R. E., (2018). *Digital image processing*. New York: Pearson.

Hausen, R., & Robertson, B. E., (2020). Morpheus: A deep learning framework for the pixel-level analysis of astronomical image data. *The Astrophysical Journal Supplement Series, 248*(20), 1–37.

Hwang, H., & Haddad, R. A., (1995) Adaptive Median Filters: New Algorithms and Results. *IEEE Transactions on Image Processing, 4*(4), 499–502.

Kandemir, C., Kalyoncu, C., & Toygar, Ö., (2015). A weighted mean filter with spatial-bias elimination for impulse noise removal, *Digital Signal Processing, 46*, 164–174.

Lu, C. T., Chen, Y. Y., Wang, L. L., & Chang, C. F., (2016). Removal of salt-and-pepper noise in corrupted image using three-values-weighted approach with variable-size window, *Pattern Recognition Letters, 80*, 188–199.

Öziç, M. Ü., & Özşen, S., (2020). Comparison global brain volume ratios on Alzheimer's disease using 3D T1 weighted MR images. *European Journal of Science and Technology*, (18), 599–606.

Pratt, W. K. (1975) Semiannual Technical Report. *Image Processing Institute*, University of Southern California.

Tukey, J. W. (1977) *Exploratory Data Analysis*, Reading, MA: Addison-Wesley.

Wang, Z., Bovik, A. C., Sheikh, H. R., Simoncelli, E. P., (2004) Image quality assessment: From error visibility to structural similarity, *IEEE Transactions on Image Processing, 13*(4), 600–612.

Weber, A. G., (1997) The USC-SIPI image database version 5. *University of Southern California, Viterbi School of Engineering, Signal and Image Processing Institute*, Los Angeles, CA, USA: USC SIPI Technical Report 315, pp. 1–24.

Zeren, M. T., Aytulun, S. K. & Kırelli, Y., (2020). Comparison of SSD and faster R-CNN algorithms to detect the airports with data set which obtained from unmanned aerial vehicles and satellite images. *European Journal of Science and Technology*, (19), 643–658.

Zhang, P., & Li, F., (2014). A new adaptive weighted mean filter for removing salt-and-pepper noise, *IEEE Signal Processing Letters, 21*(10), 1280–1283.